ACS APPLIED MATERIALS & INTERFACES

Research Article

www.acsami.org

New Design of Shape Memory Polymers Based on Natural Rubber Crosslinked via Oxa-Michael Reaction

Tengfei Lin, Siwei Ma, Yang Lu, and Baochun Guo*

Department of Polymer Materials and Engineering, South China University of Technology, Guangzhou 510640, People's Republic of China

Supporting Information

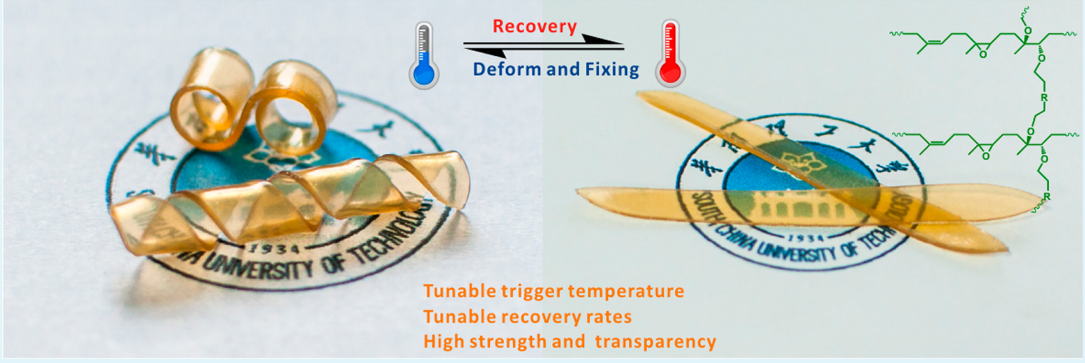

ABSTRACT: Shape memory polymers (SMPs) based on natural rubber were fabricated by crosslinking epoxidized natural rubber with zinc diacrylate (ZDA) using the oxa-Michael reaction. These SMPs possessed excellent shape fixity and recovery. The glass transition largely accounted for the fixing of the SMPs temporary shape. Increasing the ZDA content allowed the trigger temperature (20−46 °C) and recovery time (14−33 s) of the SMPs to be continuously tuned. Nanosized silica (nanosilica) was incorporated into the neat polymers to further increase the flexibility and tune the recovery stress. The nanosilica−SMPs exhibited exceptionally high strength in a rubbery state (>20 MPa). The nanosilica−SMPs exhibited high transparency, making them suitable in visible heat-shrinkable tubes.

KEYWORDS: *shape memory polymer, epoxidized natural rubber, zinc diacrylate, oxa-Michael reaction, reinforcement*

INTRODUCTION

Shape memory polymers (SMPs) are a class of smart materials. They can recover their original shape after being deformed into temporary shapes, when subjected to stimuli such as heat, light and pH.[1−4] SMPs have found applications in sensors, self-deploying sun sails in spacecraft, self-disassembling mobile phones and intelligent medical devices.[5−7] SMPs are most commonly triggered by heat.[8,9] SMPs typically consist of crosslinks that determine the permanent shape and reversible segments having a glass transition or crystalline melting transition.[10] A temporary shape can be fixed by quenching the deformed polymer network at a temperature well below the transition temperature. When the sample is reheated to above the transition temperature, the temporary shape reverts to the permanent shape because of the entropy elasticity of the polymer chains.[10] Heat-triggered SMPs may be fixed into a temporary state by the glass transition or crystallization.

Elastomer-based SMPs have been rarely reported because of their low glass transition temperature (T_g).[11−13] There have been several reports of the formation of crystallites in elastomers with low molecular weight substances. For example, fatty acids[14] and hindered phenols[15] have been blended with rubber to form SMPs. In the former, the fixing of the temporary shape is realized by the crystallization of the fatty acids. In the latter, the fixing of the temporary state is realized by the glass transition of the aggregated hindered phenols. In these two SMPs, a single elastomer is used to create a family of SMPs with different trigger temperatures, by selecting substances with appropriate melting points or glass transitions. However, if the glass transition of the elastomer could be more readily controlled by crosslinking, the elastomers themselves could be used as SMPs directly. SMPs based on epoxidized natural rubber (ENR) crosslinked by 3-amino-1,2,4-triazole have been reported.[16] In such systems, the T_g of ENR can be increased by triazole crosslinking.

We recently proposed an alternative approach for crosslinking ENR using the oxa-Michael reaction.[17] The addition of zinc acrylate (ZDA) caused the T_g of the crosslinked ENR to increase to well above room temperature. The crosslinked network then exhibited a permanent shape. The restricted chain mobility below the T_g that provided the thermally reversible, temporary network needed for the SMP.

Received: January 13, 2014
Accepted: March 27, 2014
Published: March 27, 2014

In the present study, we report the potential of the ZDA-cured ENR as a thermally-triggered SMP. The SMPs characteristics include a tunable trigger temperature and high mechanical strength, and are correlated to the structure of the ZDA-cured ENR. This study describes the design of SMPs based on elastomeric materials, and provides candidates for transparent, high strength and SMPs. These may find application in heat-shrinkable tubes for electronics, or films for packaging.

EXPERIMENTAL METHODS

Raw Materials. ENR with an epoxidation degree of 50% was produced by the Agricultural Products Processing Research Institute, Chinese Academy of Tropical Agricultural Science, Zhanjiang, P. R. China. ZDA (technically pure) was producted by the Xi'an Organic Chemical Factory, Xi'an, P. R. China. Precipitated silica (nanosized SiO_2 hereafter denoted nanosilica, VN3) with specific area of ~175 m^2/g was purchased by Evonik Degussa (P. R. China) Co., Ltd.

Preparation of ZDA-Cured ENR and the ENR/Silica Composites. ENR with different amounts of ZDA and nanosilica were mixed using an open two-roll mill. The well-mixed compounds were press-cured into 1 mm thick sheets at 160 °C × T_{c90} (where T_{c90} is the vulcanization time). The compositions of the rubber compounds are listed in Table 1.

Table 1. Composition of ZDA-Cured ENR and the ENR/Silica Composites (phr[a])

codes	EZ5	EZ10	EZ20	EZ40	EZ60
ENR	100	100	100	100	100
ZDA	5	10	20	40	60
codes	EZS10	EZS20	EZS30	EZS40	EZS50
ENR	100	100	100	100	100
ZDA	20	20	20	20	20
nanosilica	10	20	30	40	50

[a]phr: parts per 100 parts of rubber.

Measurements. The curing characteristics including the minimum torque (M_L), maximum torque (M_H), scorch time (T_{c10}) and vulcanization time (T_{c90}) of the ENR compounds were determined at 160 °C using a U-CAN UR-2030 vulcameter, Taiwan. The exact meanings of these parameters are shown in Figure 1. Dynamic mechanical analysis (DMA) was carried out a Netzsch DMA242 instrument (Germany). Testing was carried out under tension conditions, at a frequency of 1 Hz. The scanning temperature ranged from −120 to +100 °C, with a heating rate of 5 °C/min. Tensile, tear and hardness tests of the vulcanizates were performed at 25 °C, following ISO 37-2005, ISO 34-2004 and ISO 7619-2004, respectively.

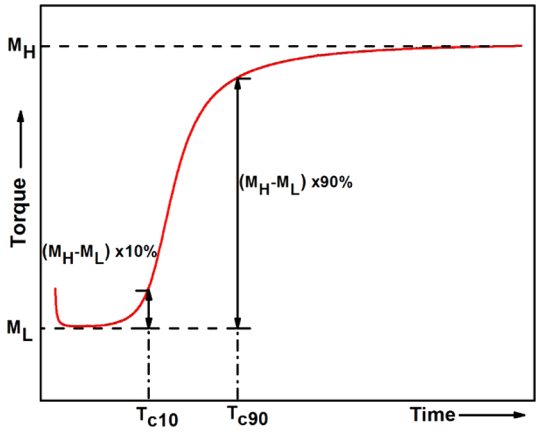

Figure 1. Typical curing profile for rubber compound.

X-ray diffraction (XRD) data were collected at ambient temperature on a Rigaku Dmax/III diffractometer, using Cu Kα radiation (λ = 1.54 Å) with an accelerating voltage and current of 40 kV and 30 mA, respectively. Samples were scanned from 4° to 60°, with a step length of 0.02° at 24 °C.

The melting and crystallization behavior of ZDA-cured ENR were determined by differential scanning calorimetry (DSC), using a TA Q20 instrument (USA). The thermal histories of the samples were eliminated by heating them to 150 °C. The samples were then cooled to −65 °C, and reheated at 10 °C/min to measure the T_g.

Tensile tests above T_g (as determined by DSC) were performed by using a TA DMA Q800 machine. After equilibrating at 20 °C above T_g for 10 min, samples were stretched at 0.5 N/min until the strain/stress limit was reached. The thicknesses of the sample sheets were ~0.2 mm. Tensile tests at elevated temperature were repeated at least three times to ensure reproducibility.

Cryogenically fractured sample surfaces were observed by scanning electron microscopy (SEM) with an EVO 18 microscopy (Germany). Energy dispersive X-ray spectra (EDS) of Zn in the ZDA-cured ENR samples were collected using an INCA 350 spectrometer (Oxford, England).

Thermomechanical cycle experiments were performed with a TA DMA Q800 instrument to characterize the shape memory behavior of ZDA-cured ENR. To eliminate the stress history during processing, samples were prestrained (involving hot-stretching then recovery) before thermomechanical cycle testing. Prior to deformation, 20.0 × 5.0 × 0.7 mm samples were heated to 20 °C above T_g, and equilibrated for 10 min. In step 1, samples were deformed by applying a progressively increasing force, from a preloaded value of 0.005 N to a designated value with a strain (ε_m), at a rate of 0.5 N/min (deformation). In step 2, samples were cooled at a rate of 3 °C/min to 20 °C below T_g under a constant force to fix the deformation (cooling). In step 3, the force exerted on the samples was unloaded to the preloaded value of 0.005 N at a rate of 0.5 N/min. This was followed by an additional 10 min isothermal step to ensure shape fixing at 30 °C below T_g (unloading and shape fixing). Upon unloading, part of the strain ($\varepsilon_m - \varepsilon_u$) was instantaneously recovered, leaving an unloading strain (ε_u). In the final step, samples were reheated at a rate of 3 °C/min to 20 °C above T_g and held there for 10 min to recover any possible residual strain (recovery). The recovery process left a permanent strain ($\varepsilon_{p(N)}$). This four-step thermomechanical cycle was repeated three times for each sample.

The shape fixity (SF) and shape recovery (SR) were defined as

$$\mathrm{SF}\ (\%) = \frac{\varepsilon_u}{\varepsilon_m} \times 100, \quad \mathrm{SR}\ (\%) = \frac{\varepsilon_m - \varepsilon_{p(N)}}{\varepsilon_m - \varepsilon_{p(N-1)}} \times 100$$

RESULTS AND DISCUSSION

Transitions in ZDA-Cured ENR and Mechanism of the SMPs. The reaction mechanism and vulcanization behavior of ZDA-cured ENR have been previously elucidated. ZDA was expected to act as a crosslinking agent and catalyst for the oxa-Michael reaction.[18,19] The two double bonds of ZDA act as crosslinking points, and Zn^{2+} in ZDA acts as the catalytic center. ZDA was also considered to be a probable catalyst for the ring-opening of ENR, as it is a carboxylate nucleophile and cation and acts as a Lewis acid catalyst in the epoxide ring-openings.[20−22] Sufficient hydroxyls groups were expected to be generated for the subsequent oxa-Michael addition between the hydroxyl group and double bond.

A dynamic analysis was conducted on vulcanized ENR containing varying amounts of ZDA. The storage modulus and loss modulus as a function of temperature are shown in Figure 2. The storage modulus and loss modulus of ZDA-cured ENR increased with increasing ZDA content. The tan δ peak

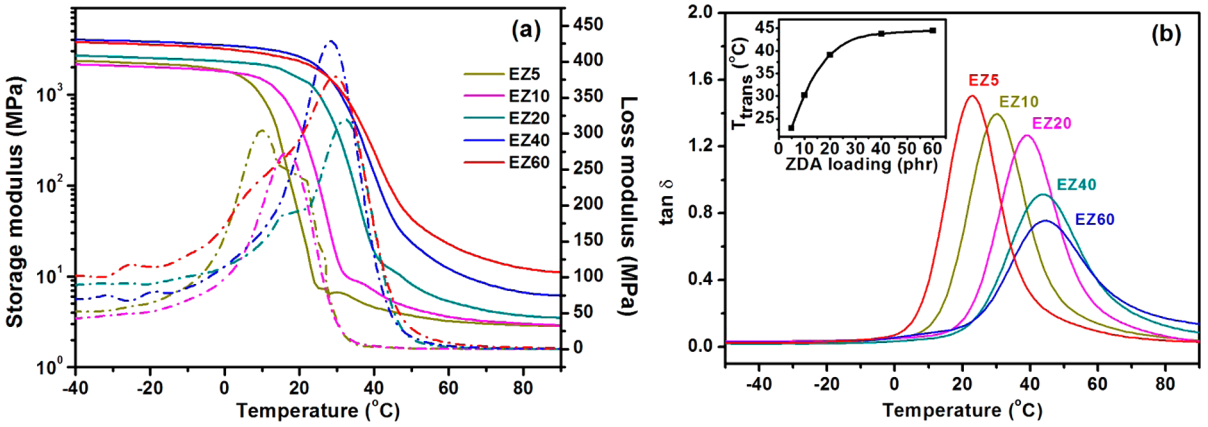

Figure 2. (a) Storage modulus (E', solid) and loss modulus (E'', dashed), and (b) tan δ of ZDA-cured ENR. Data of EZ5, EZ10 and EZ20 were sourced from the literature.[17]

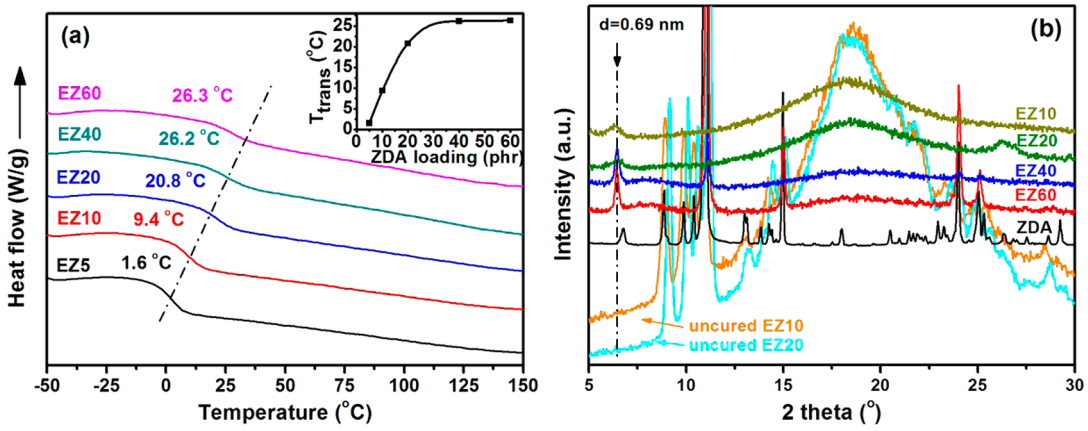

Figure 3. (a) Heat enthalpy curves of ZDA-cured ENR, as measured by DSC with a heating rate of 10 °C/min. (b) WAXD patterns of uncured and cured ENR/ZDA compounds with varying ZDA contents.

intensities of ZDA-cured ENR consistently decreased with increasing ZDA content. This suggested a continuous decrease in chain mobility, associated with an increasing crosslinking density.[17,23] A single loss factor peak was observed for all samples. The transition within the ZDA-cured ENR vulcanizates was expected to be the glass transition. T_g increased with increased ZDA content in the vulcanizates, indicating the structural confinement of rubber chains from the increased crosslinking density. T_g increased from 22.9 to 44.5 °C as the ZDA content increased from 5 to 60 phr. When nanosilica was incorporated, the storage modulus of the ENR/silica composites further increased with increased nanosilica loading (Figure S1, Supporting Information). The tan δ peask intensities of the ENR/silica composites decreased, and the loss modulus consistently increased with the nanosilica content. This suggested a continuous decrease in chain mobility. The T_g of ENR/silica composites was largely independent of nanosilica concentration, in accordance with reported results.[24,25] The modulus below the switching temperature (crystalline and/or glassy modulus) typically governs the strength of the SMP, whereas the modulus above the switching temperature (rubbery modulus) determines the recovery rate.[26] The driving force of shape recovery is the elastic force generated during deformation. A higher rubbery modulus generates a higher elastic stress and hence a faster recovery speed. Similar observations and explanations have been reported for other SMPs.[26−28] Both mechanical strength and recovery rate are important in practical applications. In the present system, the mechanical strength and recovery rate could be tuned by adjusting of the ZDA and nanosilica contents and is discussed later.

T_g values of SMPs with varying ZDA contents were also measured by DSC, and the results are shown in Figure 3a. Only a single transition was observed in the DSC results of the vulcanizates. A low ZDA concentration (5 phr) led to a low T_g of 1.6 °C, as measured by DSC. Higher ZDA contents progressively increased the T_g. The addition of 40 phr of ZDA resulted in a T_g of 26.2 °C. The transition temperatures for the shape memory behavior could therefore be tailored by adjusting the ZDA concentration.

Wide angle XRD (WAXD) patterns of the ZDA-cured samples are shown in Figure 3b, and WAXD patterns of the uncured ZDA/ENR compounds are shown for comparison. Pure ENR was amorphous. Diffractions at ∼6.77°, 11.08°, 14.97°, 24.01° and 25.05° were clearly resolved in the patterns of crystalline ZDA. Such diffractions were also observed in the patterns of the uncured ENR/ZDA compounds. This implied that ZDA retained its original crystalline structure in the compound before vulcanization. After vulcanization, these diffractions disappeared, and a new diffraction at ∼6.40° was observed. These changes were believed to be related to the chemical reaction between ENR and ZDA. During vulcanization, crystalline ZDA melted into the ENR matrix and became the crosslinking chains via oxa-Michael addition. ZDA

dx.doi.org/10.1021/am500236w | ACS Appl. Mater. Interfaces 2014, 6, 5695−5703

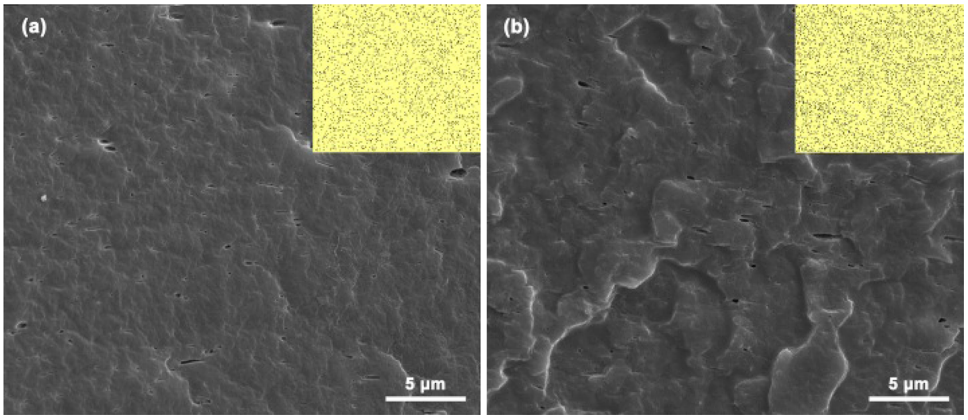

Figure 4. SEM images and EDS spectra (inset) of Zn for (a) EZ40 and (b) EZ60.

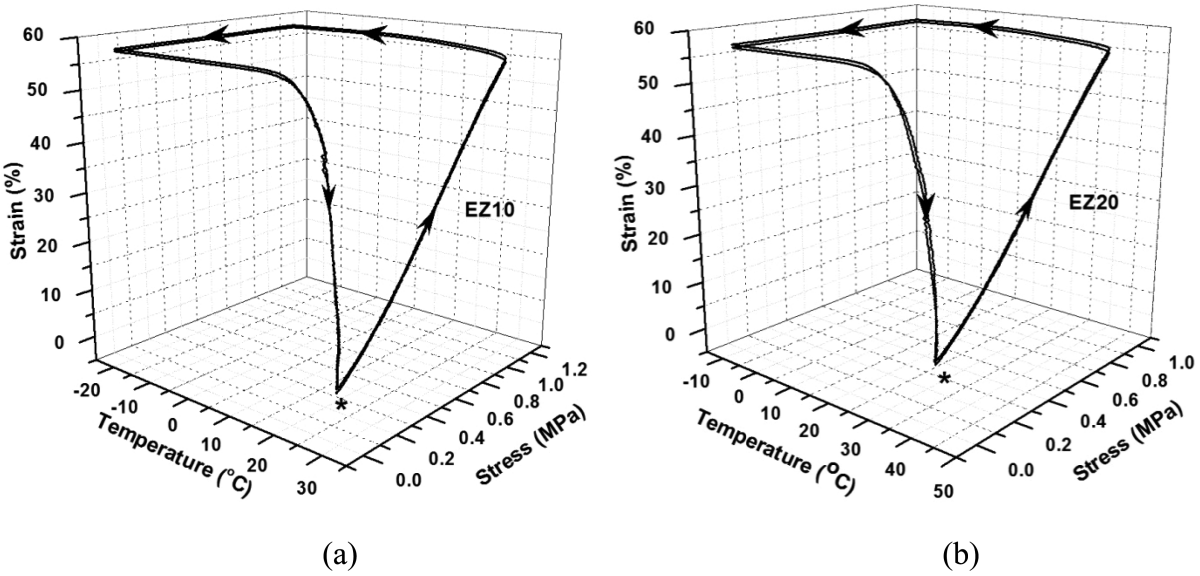

Figure 5. Stress-controlled program cycling for (a) EZ10 and (b) EZ20. An asterisk indicates beginning points for the cycling process.

was unable to recrystallize, so its initial crystal structure was lost. The new diffraction at ~6.40° may have been attributed to the formation of polyacrylic acid, which, in this system, can be formed from heating residual acrylic acid.[29] The above-mentioned diffractions were also observed for higher ZDA concentrations (60 phr), because excess ZDA was not completely used in the curing process. However, the melting of these crystallites was not observed in the DSC and DMA results. This was possibly because of the overlap of melting and the glass transition, or the low crystallite content and hence limited enthalpy for melting or crystallization. The shape fixing and memorizing capability of ZDA-cured ENR was realized by the glass transition, rather than by crystallization. The influence of nanosilica on the crystallization of the ENR/silica composite was also investigated (Figure S2, Supporting Information). The addition of nanosilica resulted in the disappearance of the diffraction at ~6.40°, suggesting a restricted formation of crystallites. Nanosilica had minimal effect on the T_g (Figure S1, Supporting Information).

Figure 4 shows SEM images and EDS spectra of Zn in ZDA-cured ENR with varying amounts of ZDA. The SEM results indicated that ZDA was well-dispersed in the ENR matrix, with very limited aggregation observed at rough interfaces. ZDA was uniformly dispersed in the ENR matrix, even at high concentrations. This was attributed to the strong chemical interaction between ENR and ZDA. During vulcanization, ENR epoxy group ring-opening occurred under the catalysis of Zn^{2+}. The oxa-Michael addition reaction between the C═C of ZDA and the epoxy group ring-opening of ENR resulted in strong interfacial interaction and well-dispersed ZDA.

The above analysis indicated that although there are some crystallites formed in the network, the trigger mechanism of the ZDA-cured ENR is practically the activation of chain mobility is actually determined by the glass transition of the crosslinked ENR. ENR chains could be extended above the T_g and fixed in a temporary shape when the chains are frozen below the T_g. Upon reheating above the T_g, the elastic entropy was released and the shape reverted to the original. The T_g was determined by the crosslink density of the network, which increased with increased ZDA content. Therefore, the trigger temperature could be tuned by the concentration of the crosslinking agent ZDA.

Shape Memory Performance of ZDA-Cured ENR. To examine the SMP performance of ZDA-cured ENR, stress-controlled program cycling of ENR cured by varying ZDA contents was performed. The results are shown in Figure 5. Shape fixity (SF) and shape recovery (SR) values are shown in Figure 6 (and Table S1, Supporting Information). Figure 6

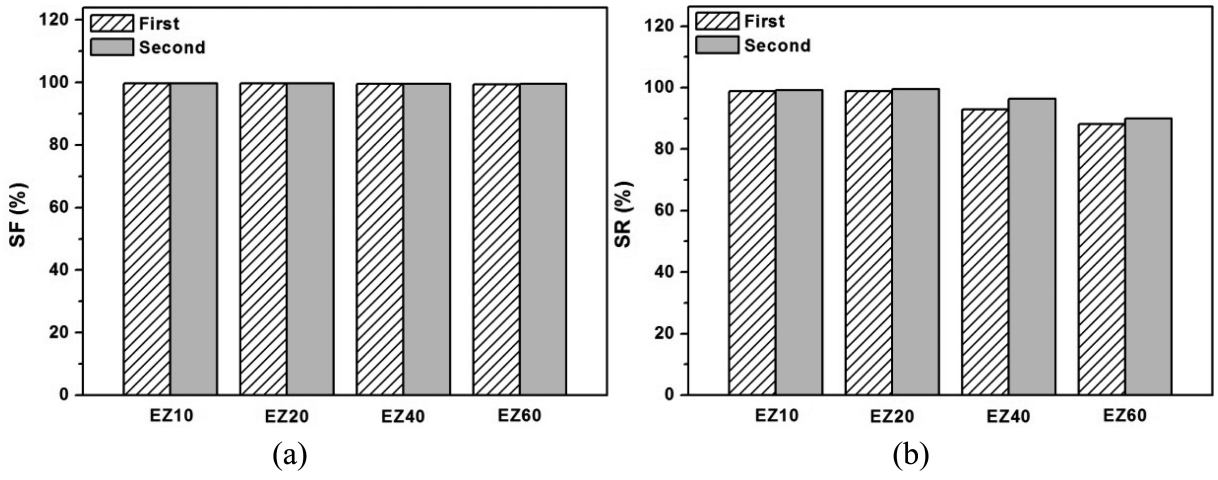

Figure 6. (a) SF and (b) SR values of ZDA-cured ENR with vary ZDA contents.

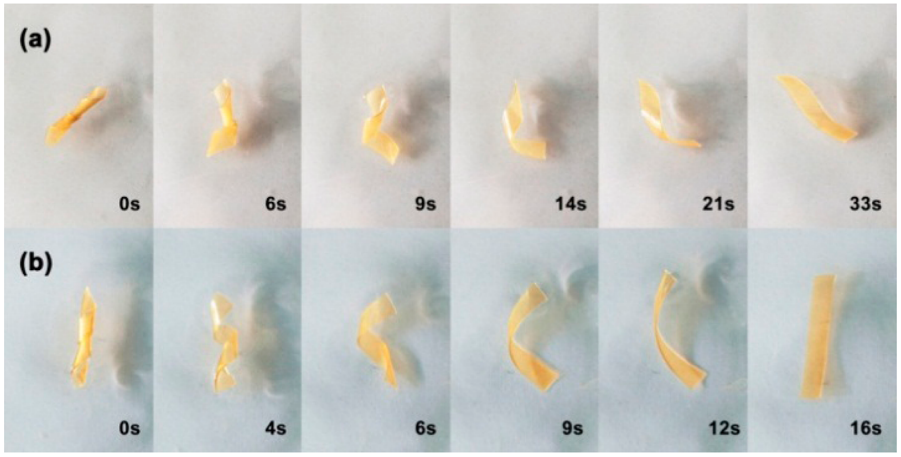

Figure 7. Transition from a temporary spiral to permanent linear shape for (a) EZ10 and (b) EZ40. Recovery was recorded after heating samples to 20 °C above the T_g.

shows that an increased ZDA loading had a minimal effect on the composites SF. The SF was also independent on the cycling time. The SR slightly decreased with increasing ZDA content and increased with cycle time. The addition of ZDA increased the composites crosslink density. However, some isolated ZDA-rich domains remained and may have slipped and permanently deformed when the sample was stretched. This effect was more significant at higher ZDA content, as shown in Figure S3 (Supporting Information). Thus, the SR of the composites slightly decreased with increased ZDA content. ZDA-rich domains rearranged in the matrix with increasing cycle time, and slipping was alleviated during cycling. This resulted in a significantly higher SR of ∼100%.

Figure 7 shows the evolution from a temporary spiral to permanent linear shape for ZDA-cured ENR. ENR cured by 10 phr of ZDA required 33 s for SR, whereas ENR cured by 40 phr of ZDA required ∼16 s. A large drop in the storage modulus around T_g is crucial for use as a SMP, according to the model proposed by Kim.[30] A high elasticity ratio, [glass-state modulus/rubbery modulus (E'_g/E'_r)], preferably with a minimum difference of two orders of magnitude, allows easy shaping at $T > T_g$, and high resistance to deformation at $T < T_g$. In the present system, all samples possessed high elasticity ratios, with differences greater than 2 orders of magnitude (Table 2). This was responsible for their favorable SF ratios.

Table 2. Mechanical Properties of ZDA-Cured ENR[a]

samples	tensile strength (MPa)	modulus at 100% strain (MPa)	strain at break (%)	tear strength (kN·m^{-1})	E'_g/E'_r[b]
EZ5	10.4 ± 0.4	1.5 ± 0.2	333 ± 5	11.8 ± 0.6	813
EZ10	12.1 ± 1.1	4.1 ± 0.3	198 ± 12	33.2 ± 1.3	709
EZ20	24.0 ± 1.7	9.2 ± 2.2	216 ± 20	64.6 ± 4.5	728
EZ40	25.8 ± 0.4	19.5 ± 0.5	148 ± 4	88.7 ± 3.4	608
EZ60	24.3 ± 0.6	21.1 ± 0.8	134 ± 11	113.3 ± 8.3	310

[a]Measured at room temperature (25 °C). [b]Determined by DMA.

The rubbery modulus of the SMP determines its recovery speed, and those with a higher rubbery modulus recover faster. The SMP with 40 phr of ZDA possessed a higher rubbery modulus than that of the SMP with 10 phr of ZDA and hence exhibited a faster SR rate. This observation is consistent with other reported systems.[31,32] The addition of nanosilica further increased the SR rate, as shown in Figure S4 (Supporting Information). The recovery time of ZDA-cured ENR could be adjusted by the ZDA or nanosilica concentrations within the SMP.

Reinforcement of ZDA-Cured ENR. To further regulate the shape memory performance, nanosilica was used to reinforce ZDA-cured ENR. The chemical interaction between ENR epoxy groups and the silanol groups on silica has been

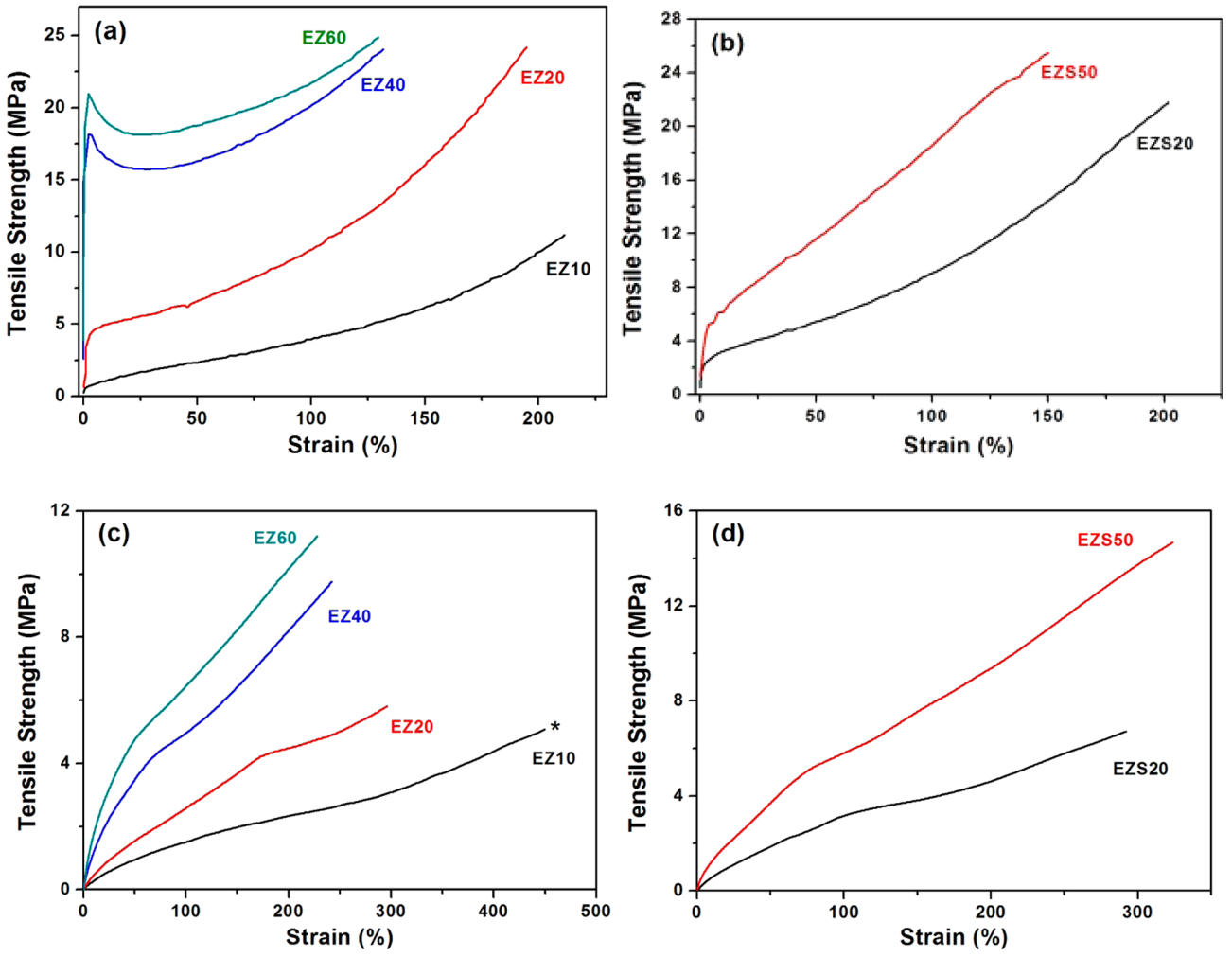

Figure 8. Tensile stress–strain curves of the composites at (a) and (b) room temperature (25 °C) and (c) and (d) elevated temperature (20 °C above the T_g). An asterisk indicates not fractured upon reaching the DMA instruments elongation limit.

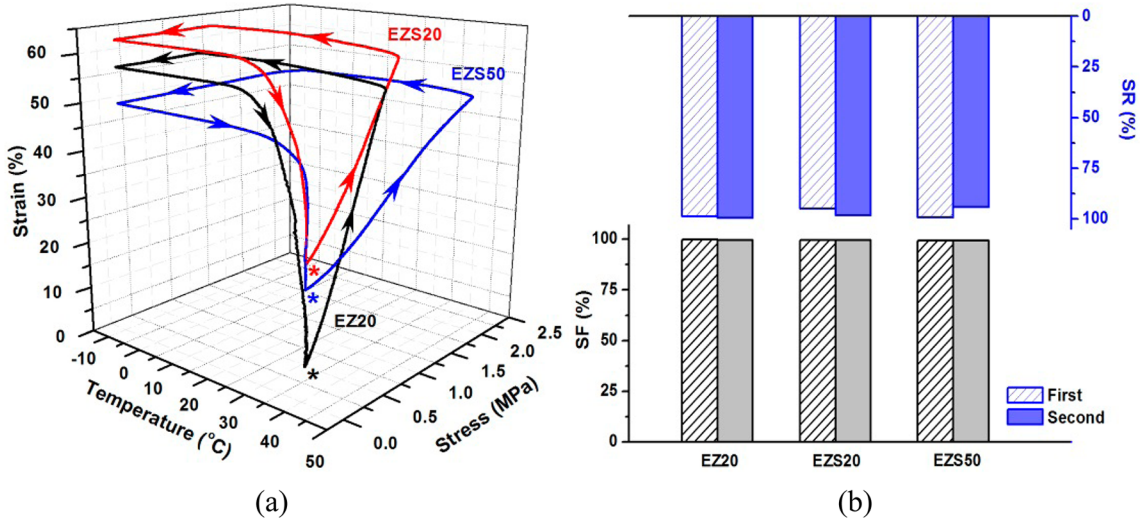

Figure 9. Stress-controlled program cycles for (a) EZ20 (black), EZS20 (red) and EZS50 (blue) and (b) their SF and SR values. An asterisk indicates beginning points for the cycling process.

reported.[33] Figure 8 shows the effect of ZDA and nanosilica content on the mechanical properties of ZDA-cured ENR vulcanizates, at below and above the T_g. Figure 8(a) shows the effect of ZDA loading on the tensile properties of ENR at room temperature. When the ZDA content was <20 phr, the crosslinked ENR behaved as a soft rubber. When the ZDA content was >40 phr, it behaved like a rigid plastics, exhibiting definite yielding. The dependence of mechanical properties on

dx.doi.org/10.1021/am500236w | ACS Appl. Mater. Interfaces 2014, 6, 5695–5703

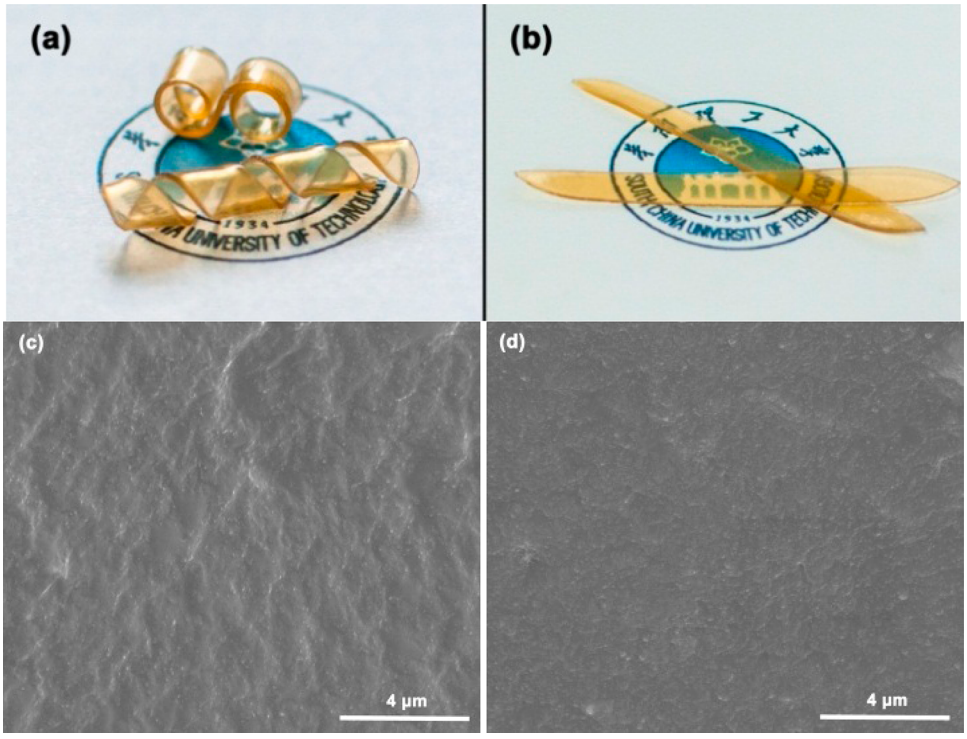

Figure 10. Optical images of EZS50 in the (a) temporary and (b) recovered shape states and SEM images of (c) EZS20 and (d) EZS50.

ZDA loading are shown in Table 2. The overall mechanical properties significantly increased with increasing ZDA loading. The modulus aslo significantly increased with increasing ZDA content. These observations also provided implications for a continuously increased T_g. The tensile strength at room temperature was well above 20 MPa, except for ENR cured with 10 phr of ZDA. When the ENR was further reinforced by nanosilica, the modulus of ENR significantly increased, although the increment in tensile strength was less pronounced, as shown in Figure 8b. The dependence of mechanical properties on nanosilica loading is shown in Figure S5 and Table S2 (Supporting Information). The tensile strength above the T_g decreased significantly, as shown in Figure 8c. The yielding at higher ZDA content was not observed, suggesting the transformation into elastomers. The tensile strength also increased with increasing ZDA content at elevated temperature. For example, with 40 phr of ZDA loading, the tensile modulus (100% strain) and tensile strength are increased to 5.0 and 9.8 MPa, respectively. These represented 233 and 92% increases on those for ENR with 10 phr of ZDA, respectively. Nanosilica further increased the tensile properties at elevated temperature, as shown in Figure 8d. The ENR/silica composite containing 50 phr of nanosilica exhibited a tensile strength of 14.7 MPa, which was 153% higher than that of the control sample without nanosilica. The significant reinforcement by nanosilica may have been attributed to its excellent dispersion. This is supported by the high transparency and SEM observations and is discussed later. It may be because of the high interfacial bonding between surface silanol and carbonyl groups. The mechanical properties of the current SMPs are much higher than reported examples.[34−36] Consequently, the ENR composites exhibited various combinations of stress and strain by adjusting the ZDA and nanosilica loading. Such SMPs may have potential in engineering as high loading actuators.

Stress-controlled thermomechanical cycling of the reinforced composites was conducted to better understand the effect of nanosilica reinforcement on SMP performance. The results are shown in Figure 9a. The SF and SR values of EZS20 and EZS50 are shown in Figure 9b (and Table S3, Supporting Information). The addition of nanosilica had no detrimental influence on the SF or SR of the composites, and the SF and SR values were independent of cycling time. The addition of nanosilica increased the modulus of the SMPs. For example, the SMP modulus (50% strain) increased to 2.3 MPa after the addition of 50 phr of nanosilica, which was 170% higher than that of the unreinforced SMP. The reinforced samples exhibited high elasticity ratios (Table S3, Supporting Information), which were responsible for their favorable SF ratios.

The nanosilica-reinforced SMPs exhibited high transparency. Figure 10a,b shows EZS50 in temporary and recovered states. SEM was used to investigate the structural origins for this transparency. Figure 10c,d shows SEM images of EZS20 and EZS50, respectively. Aggregated ZDA was not readily apparent in the SEM images, suggesting its excellent dispersion within ENR. This observation is in agreement with the above SEM results. Nanosilica was also observed to be uniformly dispersed in ENR, even at a concentration as high as 50 phr. Polar epoxy groups of ENR reportedly provide good compatibility between the rubber matrix and polar fillers including silica.[37,38] This compatibility originates largely from hydrogen bonding between surface silanol and the carbonyl groups, or ether-like moieties in the ENR network. Nanosilica can therefore be excellently dispersed in the ENR matrix. Such favorable dispersion and interaction between the ENR and nanosilica led to the improved mechanical performance of the SMP composites and their resulting high transparency.

We previously demonstrated that ZDA-cured ENR exhibited high resistance to heat/oxygen aging.[17] ZDA-cured ENR could sustain its high mechanical properties after accelerated aging for

21 days at 100 °C. However, a conventional sulfur-cured ENR lost its elasticity within 5 days. This resistance favors the SMPs use in outdoor applications, or in harsh environments such as heat-shrinkable tubes at elevated temperatures.

CONCLUSION

The feasibility of SMPs based on natural rubber was demonstrated by crosslinking ENR with ZDA via oxa-Michael addition reaction. SMPs with varying T_g values (20−46 °C) and recovery times (14−33 s) were developed from a single polymer by adjusting the ZDA concentration. The SMPs possessed excellent shape fixities and shape recoveries. The nanosilica-reinforced SMPs exhibited exceptionally high strength in the rubbery state (over 20 MPa). The ZDA and nanosilica concentration were used to tune the SMPs stress and strain. The nanosilica-filled SMPs exhibited high transparency. This makes them suitable for use in visible heat-shrinkable tubes for heated oxygen conditions.

ASSOCIATED CONTENT

Supporting Information

SMP properties (Table S1) and stress-controlled program cycling results (Figure S3) for ZDA-cured ENR, characterization of ENR/silica composites including DMA results (Figure S1), WAXD patterns (Figure S2), SMP properties (Figure S4, Table S3) and mechanical data (Figure S5, Table S2). This material is available free of charge via the Internet at http://pubs.acs.org.

AUTHOR INFORMATION

Corresponding Author

*B. C. Guo. E-mail: psbcguo@scut.edu.cn. Tel: +86 20 87113374. Fax: +86 20 22236688.

Notes

The authors declare no competing financial interest.

ACKNOWLEDGMENTS

The authors acknowledge financial support from the National Natural Science Foundation of China (Nos. 51222301 and 51333003), Research Fund for the Doctoral Program of Higher Education of China (No. 20130172110001) and Fundamental Research Funds for the Central Universities (No. 2014ZG0001).

REFERENCES

(1) Lendlein, A.; Jiang, H.; Jünger, O.; Langer, R. Light-Induced Shape-Memory Polymers. *Nature* **2005**, *434*, 879−882.
(2) Gil, E. S.; Hudson, S. M. Stimuli-Reponsive Polymers and Their Bioconjugates. *Prog. Polym. Sci.* **2004**, *29*, 1173−1222.
(3) Huang, W. M.; Yang, B.; An, L.; Li, C.; Chan, Y. S. Water-Driven Programmable Polyurethane Shape Memory Polymer: Demonstration and Mechanism. *Appl. Phys. Lett.* **2005**, *86*, 114105.
(4) Liu, Y.; Lv, H.; Lan, X.; Leng, J.; Du, S. Review of Electro-Active Shape-Memory Polymer Composite. *Compos. Sci. Technol.* **2009**, *69*, 2064−2068.
(5) Kunzelman, J.; Chung, T.; Mather, P. T.; Weder, C. Shape Memory Polymers with Built-in Threshold Temperature Sensors. *J. Mater. Chem.* **2008**, *18*, 1082−1086.
(6) Behl, M.; Lendlein, A. Shape-Memory Polymers. *Mater. Today* **2007**, *10*, 20−28.
(7) Liu, C.; Qin, H.; Mather, P. T. Review of Progress in Shape-Memory Polymers. *J. Mater. Chem.* **2007**, *17*, 1543−1558.
(8) Hao, J. K.; Weiss, R. A. Mechanically Tough, Thermally Activated Shape Memory Hydrogels. *ACS Macro Lett.* **2013**, *2*, 86−89.
(9) Lakhera, N.; Yakacki, C. M.; Nguyen, T. D.; Frick, C. P. Partially Constrained Recovery of (Meth)acrylate Shape-Memory Polymer Networks. *J. Appl. Polym. Sci.* **2012**, *126*, 72−82.
(10) Behl, M.; Zotzmann, J.; Lendlein, A. *Shape-Memory Polymers*; Springer: Berlin, 2010.
(11) Zhang, W.; Chen, L.; Zhang, Y. Surprising Shape-Memory Effect of Polylactide Resulted from Toughening by Polyamide Elastomer. *Polymer* **2009**, *50*, 1311−1315.
(12) Zhang, H.; Wang, H.; Zhong, W.; Du, Q. A Novel Type of Shape Memory Polymer Blend and the Shape Memory Mechanism. *Polymer* **2009**, *50*, 1596−1601.
(13) Koerner, H.; Price, G.; Pearce, N. A.; Alexander, M.; Vaia, R. A. Remotely Actuated Polymer Nanocomposites—Stress-Recovery of Carbon-Nanotube-Filled Thermoplastic Elastomers. *Nat. Mater.* **2004**, *3*, 115−120.
(14) Weiss, R. A.; Izzo, E.; Mandelbaum, S. New Design of Shape Memory Polymers: Mixtures of an Elastomeric Ionomer and Low Molar Mass Fatty Acids and Their Salts. *Macromolecules* **2008**, *41*, 2978−2980.
(15) Zhao, X.; Lu, Y.; Xiao, D.; Wu, S.; Zhang, L. Thermoplastic Ternary Hybrids of Polyurethane, Hindered Phenol and Hindered Amine with Selective Two-Phase Dispersion. *Macromol. Mater. Eng.* **2009**, *294*, 345−351.
(16) Chang, Y.; Mishra, J. K.; Cheong, J.; Kim, D. Thermomechanical Properties and Shape Memory Effect of Epoxidized Natural Rubber Crosslinked by 3-Amino-1,2,4-Triazole. *Polym. Int.* **2007**, *56*, 694−698.
(17) Lin, T.; Guo, B. Curing of Rubber via Oxa-Michael Reaction toward Significantly Increased Aging Resistance. *Ind. Eng. Chem. Res.* **2013**, *52*, 18123−18130.
(18) Hong, Y.; Shen, Z.; Hu, X.; Mo, W.; He, X.; Hu, B.; Sun, N. Acid-Catalyzed Intramolecular oxa-Michael Addition Reactions under Solvent-Free and Microwave Irradiation Conditions. *ARKIVOC (Gainesville, FL, U. S.)* **2009**, *14*, 146−155.
(19) Bernal, P.; Tamariz, J. Synthesis of Novel β-Functionalized α-Oximinoketones via Hetero-Michael Addition of Alcohols and Mercaptans to Enones. *Tetrahedron Lett.* **2006**, *47*, 2905−2909.
(20) Paterson, I.; Berrisford, D. J. *meso* Epoxides in Asymmetric Synthesis: Enantioselective Opening by Nucleophiles in the Presence of Chiral Lewis Acids. *Angew. Chem., Int. Ed.* **1992**, *31*, 1179−1180.
(21) Chini, M.; Crotti, P.; Flippin, L. A.; Macchia, F.; Pineschi, M. Regiochemical Control of the Ring-Opening of 1,2-Epoxides by Means of Chelating Processes. 2. Synthesis and Reactions of the Cis- and Trans-Oxides of 4-[(Benzyloxy)methyl]cyclohexene, 3-Cyclohexene-methanol, and Methyl 3-Cyclohexenecarboxylate. *J. Org. Chem.* **1992**, *57*, 1405−1412.
(22) Parker, R. E.; Isaacs, N. S. Mechanisms Of Epoxide Reactions. *Chem. Rev.* **1959**, *59*, 737−799.
(23) Perez, L. D.; Zuluaga, M. A.; Kyu, T.; Mark, J. E.; Lopez, B. L. Preparation, Characterization, and Physical Properties of Multiwall Carbon Nanotube/Elastomer Composites. *Polym. Eng. Sci.* **2009**, *49*, 866−874.
(24) Robertson, C.; Lin, C.; Bogoslovov, R.; Rackaitis, M.; Sadhukhan, P.; Quinn, J.; Roland, C. Flocculation, Reinforcement, and Glass Transition Effects in Silica-Filled Styrene-Butadiene Rubber. *Rubber Chem. Technol.* **2011**, *84*, 507−519.
(25) Arrighi, V.; McEwen, I.; Qian, H.; Serrano Prieto, M. The Glass Transition and Interfacial Layer in Styrene-Butadiene Rubber Containing Silica Nanofiller. *Polymer* **2003**, *44*, 6259−6266.
(26) Zhang, C. S.; Ni, Q. Q. Bending Behavior of Shape Memory Polymer Based Laminates. *Compos. Struct.* **2007**, *78*, 153−161.
(27) Jeong, H.; Lee, J.; Lee, S.; Kim, B. Shape Memory Polyurethane Containing Mesogenic Moiety. *J. Mater. Sci.* **2000**, *35*, 279−283.
(28) Merline, J. D.; Nair, C. R.; Gouri, C.; Shrisudha, T.; Ninan, K. Shape Memory Characterization of Polytetra Methylene Oxide/Poly (Acrylic Acid-co-Acrylonitrile) Complexed gel. *J. Mater. Sci.* **2007**, *42*, 5897−5902.
(29) Yu, Q.; Wang, X.; Shen, Y.; Tao, Y.; Xie, A. Preparing and Physicochemical Properties of Microcrystalline Polyacrylic Acid Gels. *Russ. J. Phys. Chem. A* **2013**, *87*, 2100−2104.

(30) Kim, B. K.; Lee, S. Y.; Xu, M. Polyurethanes Having Shape Memory Effects. *Polymer* **1996**, *37*, 5781−5793.
(31) Guo, W.; Kang, H.; Chen, Y.; Guo, B.; Zhang, L. Stronger and Faster Degradable Biobased Poly(Propylene Sebacate) as Shape Memory Polymer by Incorporating Boehmite Nanoplatelets. *ACS Appl. Mater. Interfaces* **2012**, *4*, 4006−4014.
(32) Hu, J. W.; Li, M. W.; Zhang, M. Q.; Xiao, D. S.; Cheng, G. S.; Rong, M. Z. Preparation of Binary Conductive Polymer Composites with very Low Percolation Threshold by Latex Blending. *Macromol. Rapid Comm.* **2003**, *24*, 889−893.
(33) Manna, A. K.; Bhattacharyya, A.; De, P.; Tripathy, D.; De, S.; Peiffer, D. G. Effect of Silane Coupling Agent on the Chemo-rheological Behaviour of Epoxidised Natural Rubber Filled with Precipitated Silica. *Polymer* **1998**, *39*, 7113−7117.
(34) Pan, Y.; Liu, T.; Li, J.; Zheng, Z. H.; Ding, X. B.; Peng, Y. X. High Modulus Ratio Shape-Memory Polymers Achieved by Combining Hydrogen Bonding with Controlled Crosslinking. *J. Polym. Sci., Polym. Phys. Ed.* **2011**, *49*, 1241−1245.
(35) Han, Y.; Bai, T.; Liu, Y.; Zhai, X.; Liu, W. Zinc Ion Uniquely Induced Triple Shape Memory Effect of Dipole−Dipole Reinforced Ultra-High Strength Hydrogels. *Macromol. Rapid Comm.* **2012**, *33*, 225−231.
(36) Dong, J.; Weiss, R. A. Shape Memory Behavior of Zinc Oleate-Filled Elastomeric Ionomers. *Macromolecules* **2011**, *44*, 8871−8879.
(37) Xu, H.; Liu, J.; Fang, L.; Wu, C. In Situ Grafting onto Silica Surface with Epoxidized Natural Rubber via Solid State Method. *J. Macromol. Sci., Part B: Phys.* **2007**, *46*, 693−703.
(38) Luo, Y. Y.; Wang, Y. Q.; Zhong, J. P.; He, C. Z.; Li, Y. Z.; Peng, Z. Interaction Between Fumed-Silica and Epoxidized Natural Rubber. *J. Inorg. Organomet. Polym. Mater.* **2011**, *21*, 777−783.